BIOCHEMISTRY
including biophysical chemistry & molecular biology

Article

pubs.acs.org/biochemistry

The Physical Basis of FGFR3 Response to *fgf1* and *fgf2*

Fenghao Chen and Kalina Hristova*

Department of Materials Science and Engineering, Johns Hopkins University, Baltimore, Maryland 21218, United States

ABSTRACT: Fibroblast growth factors (*fgf*s) play important roles in embryonic development and in adult life by controlling cell proliferation, differentiation, and migration. There are 18 known *fgf*s which activate four fibroblast growth factor receptors (FGFRs), with different isoforms due to alternative splicing. The physical basis behind the specificity of the biological responses mediated by different *fgf*-FGFR pairs is currently unknown. To gain insight into the specificity of FGFR3c, a membrane receptor which is critical for bone development, we studied, analyzed, and compared the activation of FGFR3c over a wide range of *fgf1* and *fgf2* concentrations. We found that while the strength of *fgf2* binding to FGFR3c is lower than the strength of *fgf1* binding, the *fgf2*-bound dimers exhibit higher phosphorylation of the critical tyrosines in the activation loop. As a result, *fgf1* and *fgf2* elicit a similar FGFR3c response at low, but not at high, concentrations. The results demonstrate the versatility of FGFR3c response to *fgf1* and *fgf2* and highlight the complexity in *fgf* signaling.

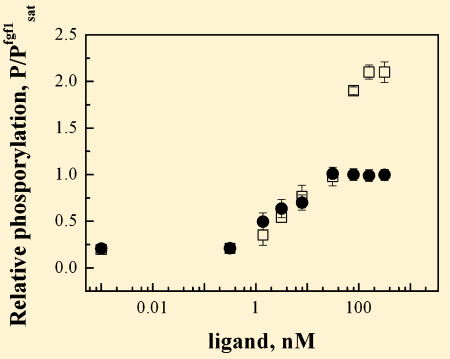

There are 18 known fibroblast growth factors, which bind to and activate four related receptor tyrosine kinases, FGFR1 through FGFR4.[1−3] These growth factors play important roles in embryonic development and in adult life by controlling cell proliferation, differentiation, and migration. The first two growth factors, *fgf1* and *fgf2*, were identified in the late 1970s, based on their ability to promote proliferation of fibroblasts in vivo.[4−7] They work in paracrine fashion, i.e., influencing the signaling of neighboring cells from a distance, and are secreted from cells in a way that is not completely understood. Both *fgf1* and *fgf2* do not have cleavable signal peptides and are exported out in a way that is independent of the ER-Golgi machinery.[8,9]

Fibroblast growth factors were demonstrated to bind heparin and heparan sulfate,[10] which is required for *fgf*/FGFR-mediated signaling.[11−13] Now it is well established that 2 FGFRs, 2 *fgf*s, and 1 heparan sulfate molecule form a stable signaling-competent dimer.[14−16] The two catalytic domains in the dimer are positioned in close proximity, and their orientation allows them to cross-phosphorylate each other.[1]

The FGF receptors belong to the large receptor tyrosine kinase (RTK) superfamily. They consist of extracellular ligand-binding domains with three immunoglobulin (Ig) like motifs (D1-D3), single TM domains, and intracellular domains composed of a kinase and regulatory sequences. There are different tissue-specific FGFR isoforms due to alternative splicing in the intracellular and extracellular domains.[2,17,18] The very presence of 18 ligands and 4 receptors, with different isoforms due to alternative splicing, gives the option of diverse response and regulation. Indeed, research thus far has established differences in binding affinities of different *fgf*s to FGFRs.[16,19,20] *Fgf1* is known as a universal ligand, capable of activating all FGFRs, while the others, including *fgf2*, exhibit various degrees of specificity.[21,22] In addition to differences in affinities,[16,19] differences in structure of ligand-extracellular domain complexes have been reported, and these differences are believed to influence the specificity of the biological response of a particular FGFR isoform.[15,23] Yet, it is not yet known how the specific biological response of a receptor is achieved upon stimulation with a particular ligand.

Here we focus on the third member of the FGFR family, FGFR3. FGFR3 has two membrane-bound isoforms, produced via alternative splicing: isoform "b", expressed in epithelial cells, and isoform "c", expressed in mesenchymal cells. FGFR3c is critical for the development of the long bones by mediating pro-differentiation signals in chondrocytes, which are of mesenchymal lineage. Deregulation of FGFR3c signaling leads to disorders of long bone development and gives rise to dwarfism phenotypes of different severity, such as achondroplasia (ACH), thanatophoric dysplasia (TD), and hypochondroplasia (HCH).[24−27] Because of its involvement in human growth disorders, FGFR3c signaling, including the response to *fgf1* and *fgf2*, has been a topic of intensive research.[21,28−38] For instance, it has been shown that BaF3 cells expressing FGFR3c exhibit similar mitogenic activity in response to *fgf1* and *fgf2*.[21] However, a pronounced difference in binding of *fgf1* and *fgf2* to FGFR3c has been observed.[16,20,39] This discrepancy suggests that ligand binding strength is not the only factor that regulates FGFR3c ligand-dependent activation. To gain further insight into this issue, we studied, analyzed, and compared the activation of FGFR3 over a wide range of *fgf1* and *fgf2* concentrations. Our findings demonstrate a different signaling capacity of FGFR3/*fgf1* and FGFR3/*fgf2* dimers, emphasizing the complexity in *fgf* signaling.

Received: June 27, 2011
Revised: September 3, 2011
Published: September 6, 2011

MATERIALS AND METHODS

Western Blots. The wild-type FGFR3 plasmid in the pcDNA 3.1+ vector was a generous gift from D. J. Donoghue at UCSD. Human Embryonic Kidney 293 T cells were transfected with the plasmid using Fugene 6 (Roche) according to the manufacturer's protocol. Cells were cultured in normal medium for 24 h following transfection and then starved in serum-free medium for 24 h. The effect of ligand was tested by incubating the cells in medium supplemented with *fgf1* or *fgf2* (Millipore, MA). Proteins from the cell lysates of HEK 293T cells were probed with a FGFR3 (H-100) antibody (sc-9007, Santa Cruz Biotechnology) or phospho-Tyr-FGFR antibody (anti-Y653/654, Cell Signaling Technology), followed by anti-rabbit HRP conjugated antibodies (W4011, Promega).

Cross-Linking. In cross-linking experiments, dimeric receptors were cross-linked with a membrane impermeable linker (BS^3, Pierce). After 24 h starvation, cells were incubated with 2 mM cross-linker for 30 min to 1 h at room temperature and then quenched in 20 mM Tris-HCl for 15 min. After two rinses with ice-cold PBS, the cells were lysed and the receptors were detected using Western blotting. The cross-linked fraction was calculated as $S_D/S = S_D/(S_M + S_D)$, where S_D is the intensity of the dimeric band and S_M is the intensity of the monomeric band.

Titration with *fgf1*. HEK 293 T cells were cultured in normal medium for 24 h following transfection and then starved in serum-free medium for 24 h. Different concentrations of *fgf1* and *fgf2* (Millipore, MA), ranging from 5 to 5000 ng/mL, were added to the serum-free medium. After incubating for 10 min with ligand, cells were lysed as described above and analyzed using Western blotting.

Quantification of Western Blots. The Western blot films were scanned and processed with ImageQuant TL. At least three sets of independent experiment were performed in order to determine the averages and the standard errors. The loading on the gels was adjusted such that all the band intensities were within the so-called linear regime and the staining intensities were proportional to the protein concentrations.[40]

A PHYSICAL–CHEMICAL DESCRIPTION OF FGFR3 ACTIVATION

Model. A simple model of RTK activation, described recently,[31] assumes that the activation is a two-step process involving ligand-independent dimerization followed by ligand binding to the unliganded dimer:

$$M + M \overset{K_1}{\leftrightarrow} d \tag{1}$$

$$d + L_2 \overset{K_2}{\leftrightarrow} D \tag{2}$$

Here, M denotes the monomer, while d and D denote the unliganded and liganded FGFR3c dimers, respectively. The ligand in this model is predimerized on heparan sulfates on the cell surface prior to binding to the unliganded dimer.[17,41] The two reactions (1) and (2) are coupled: ligand binding depletes the unliganded dimers, and this in turn decreases the monomer concentrations. The reaction constants, K_1 and K_2, are defined as follows:

$$K_1 = [d]/[M]^2 \tag{3}$$

and

$$K_2 = [D]/[L_2][d] \tag{4}$$

The mass balance equations for the total ligand concentration [TL] and the total receptor concentration [TR] are:

$$[TL] = 2[L_2] + 2[D] \tag{5}$$

$$[TR] = [M] + 2[d] + 2[D] \tag{6}$$

As shown in detail in ref 31, these four equations (3) through (6) can be solved as a function of the reaction constants K_1 and K_2 and the total ligand and receptor concentrations, [TL] and [TR], yielding [M], [d], and [D]. In particular, the concentration of monomeric receptors [M] is the solution of the following equation:[31]

$$2K_1^2K_2[M]^4 + K_1K_2[M]^3 + [K_1K_2[TL] + 2K_1 - K_1K_2[TR]][M]^2 + [M] - [TR] = 0 \tag{7}$$

This equation has a single real positive root.[31] Once [M] is determined, [d] is calculated using eq 8:

$$[d] = K_1[M]^2 \tag{8}$$

and [D] is calculated using eq 9:

$$[D] = \frac{1}{2}([TR] - [M] - 2[d]) \tag{9}$$

In this model, the concentration of phosphorylated receptors is then calculated according to[31]

$$[P] = 2\Phi_d[d] + 2\Phi_D[D] \tag{10}$$

where Φ_d and Φ_D are the probabilities for receptor phosphorylation within the unliganded and liganded dimers, respectively.

The model predicts that all receptors are liganded and dimeric at high ligand concentration, such that the phosphorylation reaches saturation above a threshold concentration, remaining constant as more ligand is added. At saturating ligand concentrations, $2[D]_{sat} = [TR]$ and therefore

$$[P]_{sat} = 2\Phi_D[D]_{sat} = \Phi_D[TR] \tag{11}$$

The phosphorylated fraction of receptors $[P]/[P]_{sat}$ is given by[31]

$$\frac{[P]}{[P]_{sat}} = \frac{2\Phi_d}{\Phi_D}\frac{[d]}{[TR]} + \frac{2\Phi_D}{\Phi_D}\frac{[D]}{[TR]} = \frac{\Phi_d}{\Phi_D}\frac{2[d]}{[TR]} + \frac{2[D]}{[TR]} \tag{12}$$

The ratio of Φ_d and Φ_D is

$$\frac{\Phi_d}{\Phi_D} = \frac{[P]_0}{[P]_{sat}} \Big/ \frac{[d]_0}{[D]_{sat}} \tag{13}$$

where $[P]_0/[P]_{sat}$ and $[d]_0/[D]_{sat}$ are the phosporylated receptor fraction and dimeric receptor fraction in the absence of ligand.

At zero ligand, eq 12 reduces to

$$\frac{[P]_0}{[P]_{sat}} = \frac{2\Phi_d}{\Phi_D}\frac{[d]_0}{[TR]} \quad (14)$$

Measurable Quantities. The phosphorylation [P] at various ligand concentrations can be measured on Western blots using antibodies that are specific for phosphorylated tyrosines. $[P]_0$ is the phosphorylation measured in the absence of ligand, while $[P]_{sat}$ is the phosphorylation measured at saturating ligand concentration. Thus, the ratio $[P]/[P]_{sat}$, given by eq 12, can be measured over a wide range of ligand concentrations, including zero ligand ($[P]_0/[P]_{sat}$). The measured $[P]/[P]_{sat}$ can be then fitted to the theoretical prediction given by eq 12, after substituting parameters from eqs 8, 9, and 13. The predicted values of $[P]/[P]_{sat}$ depend on the two unknown parameters, K_1 and K_2, which can be optimized in the fit.

The theoretical prediction of $[P]/[P]_{sat}$ also depends on the value of $[d]_0/[D]_{sat}$, the dimeric fraction at zero ligand (see eq 13). Since dimeric fraction are difficult to measure directly,[31] here we approximate dimeric fractions with the ratio of cross-linked fractions at zero ligand and at saturating ligand concentrations (thus assuming that the efficiency for cross-linking the two receptors in the dimer is not affected by the bound ligand[31]).

RESULTS

Phosphorylation of FGFR3/*fgf2* Dimers Is Higher Than the Phosphorylation of FGFR3/*fgf1* Dimers. We have previously demonstrated the successful plasma membrane expression of FGFR3c in HEK 293 T cells.[42] Here we investigated how FGFR3c responds to the ligands *fgf1* and *fgf2*. After transfection, HEK 293T cells were cultured for 24 h, starved for 24 h to induce accumulation of receptors on the plasma membrane,[35] and treated with *fgf1* or *fgf2* (Millipore, MA) at concentrations ranging from 5 to 5000 ng/mL. After incubating with the ligands for 10 min, the cells were lysed and the lysates were analyzed by Western blot. Total FGFR3 expression was probed by Western blots using anti-FGFR3 antibodies (H-100, Santa Cruz). The phosphorylation of FGFR3 was probed using antiphospho-FGFR antibodies (anti-Y653/654, Cell Signaling Technology).[31] These antibodies are specific for two phosphorylated tyrosines in the activation loop of FGFR3, Y647, and Y648. The phosphorylation of these two tyrosines is required for the activation of the kinase domain and the phosphorylation of other intracellular tyrosine residues.[43]

Representative Western blot experiments are shown in Figure 1. We observe two bands corresponding to the intermediate, 120 kDa Endo H-sensitive FGFR3c found in the ER/cis-Golgi, and the fully glycosylated mature 130 kDa FGFR3, located predominantly on the plasma membrane.[31,44] In this work dedicated to ligand binding, we focus at the mature FGFR3c 130 kDa form located predominantly on the cell surface. This is the form that has access to the ligand and thus responds to it. The lower molecular weight FGFR3c located in the ER (120 kDa band) is not exposed to ligands and is not considered in the analysis.

The activation model, given by eqs 3−13, predicts a threshold ligand concentration above which all receptors that are exposed to ligand are in their liganded dimeric state.[31] Consistent with this prediction, we see saturation in FGFR3c phosphorylation above the ligand concentration of 1000 ng/mL: phospho-staining levels stay at their constant maximum values and are not further increased when more ligand is added. As discussed previously, the Western blot protocols that we use ensure that the band intensities are always within the so-called linear range; i.e., the band intensities are proportional to the receptor concentrations.[38,40] Under these conditions the saturation we observe is not an experimental artifact, but a true saturation in receptor phosphorylation.

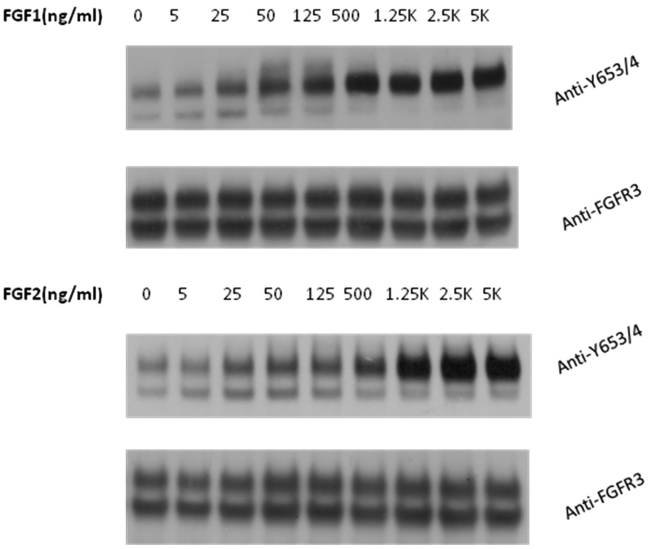

Figure 1. Western blots, showing FGFR3c phosphorylation and expression, as a function of *fgf1* concentration (A) and *fgf2* concentration (B). In these experiments, HEK 293 T cells were transfected with 1 μg of DNA encoding FGFR3c, using Fugene 6 (Roche). Twenty-four hours later, cells were starved in serum-free medium for another 24 h. They were stimulated with different concentrations of *fgf1* and *fgf2*, ranging from 5 to 5000 ng/mL, lysed, and analyzed.

Figure 1 compares the results when cells expressing FGFR3c were treated with different concentrations of *fgf1* (top) and *fgf2* (bottom). To be able to carry out a comparison of FGFR3c response to different concentrations of the two ligands, the lysates were loaded onto two gels, and the proteins in the two gels were transferred simultaneously onto a blotting membrane and incubated with antibodies. In Figure 1 we see that while the bands at zero ligand are very similar, FGFR3c phosphorylation at saturating *fgf2* concentration, $[P]_{sat}^{fgf2}$, is higher than the phosphorylation at saturating *fgf1* concentration, $[P]_{sat}^{fgf1}$. Quantification of the 130 kDa mature FGFR3c bands in the plateau region (corresponding to ligand concentration above 1000 ng/mL) yielded the value of $[P]_{sat}^{fgf1}$, obtained by averaging the results above 1250 ng/mL *fgf1*, as well as the average value of $[P]_{sat}^{fgf2}$. The ratio of $[P]_{sat}^{fgf2}/[P]_{sat}^{fgf1}$ was calculated as 2.1. Two additional independent experiments were performed (gels not shown), and the average value for the ratio $[P]_{sat}^{fgf2}/[P]_{sat}^{fgf1}$ from the three experiments was determined as 2.1 ± 0.6. To confirm this result, we reran lysates for saturating *fgf1* and *fgf2* concentrations (5000 ng/mL) on one gel (Figure 2). The side-by-side comparison confirms that FGFR3c phosphorylation is higher at saturating *fgf2* concentrations than at saturating *fgf1* concentrations, and the ratio $[P]_{sat}^{fgf2}/[P]_{sat}^{fgf1}$ is 2.0 ± 0.01.

The phosphorylation at saturating ligand concentration is related to the receptor phosphorylation probability within the liganded dimers, Φ_D, according to eq 11. The ratio $[P]_{sat}^{fgf2}/$

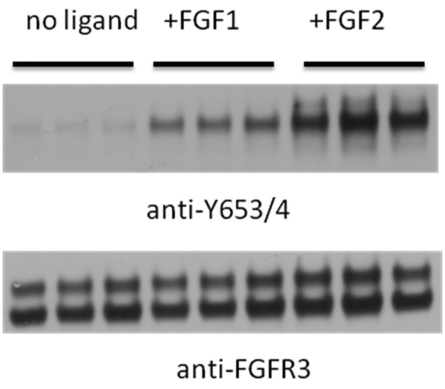

Figure 2. Side-by-side comparison of phosphorylation levels in the absence of ligand and at saturating *fgf1* and *fgf2* concentrations (5000 ng/mL).

$[P]_{sat}^{fgf1}$ is therefore equal to

$$\frac{[P]_{sat}^{fgf2}}{[P]_{sat}^{fgf1}} = \frac{\Phi_D^{fgf2}}{\Phi_D^{fgf1}}\frac{[TR]}{[TR]} = \frac{\Phi_D^{fgf2}}{\Phi_D^{fgf1}}$$

Thus, $\Phi_D^{fgf2}/\Phi_D^{fgf1} = 2.0 \pm 0.01$; i.e., the probability for receptor phosphorylation at Y647/8 within the *fgf2*-bound FGFR3c dimers is twice as high as the receptor phosphorylation probability at Y647/8 within the *fgf1*-bound FGFR3c dimers.

To measure how the phosphorylation changes as a function of ligand concentration, we quantified the anti-Y653/4 band intensities for the 130 kDa mature fully glycosylated form, for all studied ligand concentrations, for the representative experiment shown in Figure 1 and for the two additional independent experiments. The average values of the phosphorylated fractions as a function of ligand concentration are shown in Figures 3 and 5. In Figure 3, all the data, together

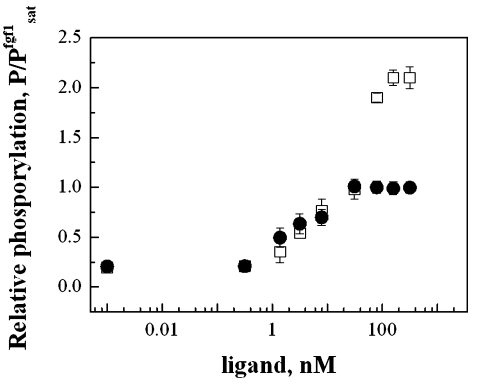

Figure 3. Receptor phoshorylation as a function of *fgf1* (solid circles) and *fgf2* (open squares) concentration. Data are from three independent Western blot experiments. The phosphorylation is assigned a value of 1 at saturating *fgf1* concentrations.

with the standard errors, are plotted on a common scale, with the value of $[P]_{sat}^{fgf1}$ set as 1. In Figure 5, the data for *fgf1* and *fgf2* are replotted on separate scales, after normalizing the two data sets separately such that the plateau level is set to 1 in both cases.

FGFR3c Cross-Linking Propensities Are Similar at Saturating *fgf1* and *fgf2* Concentrations. Next we performed cross-linking experiments at zero ligand and at saturating *fgf1* and *fgf2* concentrations (Figure 4). Cells were

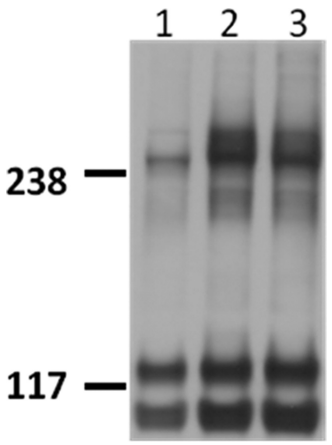

Figure 4. Western blots of cross-linked FGFR3c, in the absence of ligand and in the presence of saturating *fgf1* and *fgf2* concentrations. Cells were incubated with BS3 cross-linking agent (Pierce) for 30 min at room temperature prior to lysis. The blot was stained with anti-FGFR3 antibodies. Lane 1: no ligand; lane 2: 2500 ng/mL *fgf1*; lane 3: 2500 ng/mL *fgf2*.

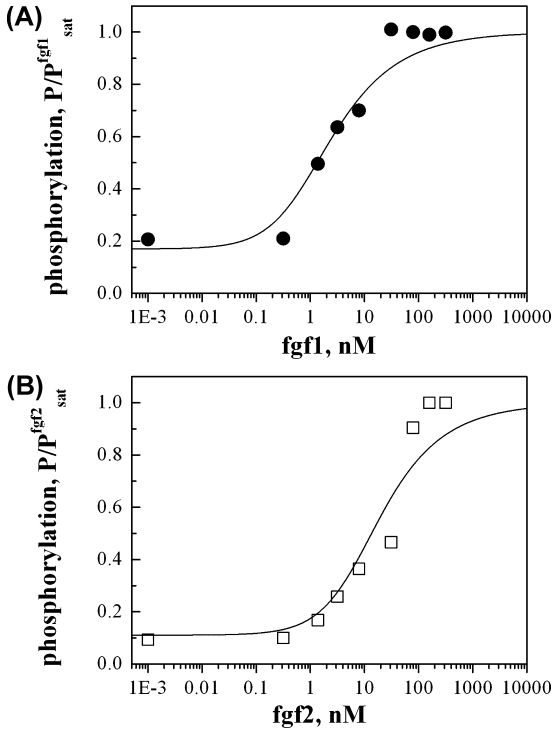

Figure 5. Fits of the RTK activation model, given by eqs 3−13, to the Western blot data. Phosphorylated fractions in the presence of *fgf1* and *fgf2* were obtained from Western blots such as the one shown in Figure 3. (A) Results from the *fgf1* titration experiments, with phosphorylation at saturating *fgf1* concentration assigned a value of 1. (B) Results from the *fgf2* titration experiments, with phosphorylation at saturating *fgf2* concentration assigned a value of 1. The two data sets were fitted independently. The two reaction constants, K_1 and K_2, were varied to achieve the best fit to the data. Fit results are shown in Table 1.

starved for 24 h and then split into three pools; no ligand was added to the first cell pool, while *fgf1* and *fgf2* at 2500 ng/mL were added to the second and third pool, respectively. A membrane-impermeable cross-linker was used, such that only the mature 130 kDa FGFR3c on the surface was cross-linked.

dx.doi.org/10.1021/bi200986f | *Biochemistry* 2011, 50, 8576–8582

FGFR3c was detected on Western blots using anti-FGFR3 antibodies (Figure 4). In the absence of ligand, we see a weak band at twice the molecular weight of mature FGFR3c (~260 kDa), corresponding to cross-linked FGFR3c. The intensity of the cross-linked band increases in the presence of saturating ligand concentrations. We quantified the bands corresponding to monomeric and cross-linked FGFR3 and determined the fraction of cross-linked FGFR3c as $S_D/S = S_D/(S_M + S_D)$, where S_D is the intensity of the dimeric band and S_M is the intensity of the monomeric 130 kDa band. From four independent experiments, we find that the cross-linked FGFR3c fraction is 0.20 ± 0.03 in the absence of ligand, 0.59 ± 0.08 in the presence of *fgf1*, and 0.51 ± 0.06 in the presence of *fgf2*.

As discussed above, we expect that all 130 kDa receptors are dimeric at saturating ligands concentrations. Yet, only about 55% of the 130 kDa form is cross-linked at saturating ligand concentrations. While it is possible that not all receptors are dimeric, it is more likely that the cross-linker has a cross-linking efficiency lower than 100% (as can be expected for the yield of any chemical reaction). For instance, the data at saturating ligand concentration are consistent with ~100% dimer and about 55% cross-linking efficiency.

We see that the cross-linked fractions at saturating *fgf1* and *fgf2* concentrations are similar (~55%). Assuming that cross-linking correlates with dimerization, we conclude that the dimeric fractions are also similar. Thus, the cross-linking data are consistent with the idea that the difference in phosphorylation that we observe in Figure 2 can be attributed to differences in phosphorylation within the liganded dimers, Φ_D. Furthermore, we can estimate the dimeric fraction at zero ligand (needed to calculate Φ_d/Φ_D according to eq 11) as the ratio of cross-linked fractions at zero ligand and at saturating ligand concentration: $[d]_0/[D]_{sat}^{fgf1} = [d]_0/[D]_{sat}^{fgf2} = 0.36 \pm 0.1$.

***fgf1* Binding to FGFR3c Is Stronger Than *fgf2* Binding.** The constant K_2 in eq 4 is a measure, albeit indirect, of the strength of ligand binding. K_2 can be determined by fitting the model given by eqs 3−13 once the ratios $[P]_0/[P]_{sat}$, $[d]_0/[D]_{sat}$, and Φ_d/Φ_D are calculated. The value of $[d]_0/[D]_{sat}$ was estimated based on cross-linking as described above, and the value of $[P]_0/[P]_{sat}$ is given by the first experimental point in Figure 3. From eq 13, we calculate $\Phi_d/\Phi_D^{fgf1} = 0.6 \pm 0.2$. Because $\Phi_D^{fgf2}/\Phi_D^{fgf1} = 2.0 \pm 0.01$, we obtain $\Phi_d/\Phi_D^{fgf2} = 0.3 \pm 0.1$.

We determined the receptor concentration [TR] by comparing the expression of the 130 kDa FGFR3c in our experiments to FGFR3c expression in the stable HEK293-fWT line, estimated to have 8.4×10^5 copies of mature FGFR3c per cell.[31] The transient expression achieved in our experiments was 21 ± 5% of the stable expression, as determined via a direct expression comparison on a Western blot (results not shown).

Using the above values, the activation model given by eqs 3−13 was fitted to the experimental data in Figure 5 using a Matlab code, yielding the optimal values of K_1 and K_2. Initial guesses for K_1 and K_2 were inputted into the Matlab code, which calculated [d], [D], [M], and the phosphorylated FGFR3c fraction, $[P]/[P]_{sat}$. This prediction was compared to the experimentally determined phosphorylated fractions and the two unknowns K_1 and K_2 were varied until the calculated predictions of $[P]/[P]_{sat}$ provided the best description of the experimental data. The optimal parameters, which did not depend on the initial guesses, are shown in Table 1.

The parameter K_2 describes the strength of ligand binding to the "preformed" unliganded dimer. The reciprocal value, $1/K_2$, is a measure of the apparent dissociation constant, in nanomolar units. Table 1 shows that the apparent dissociation constant for *fgf2* is an order of magnitude higher than the apparent dissociation constant for *fgf1*. Thus, the binding strength of *fgf1* to FGFR3c is an order of magnitude higher than the strength of *fgf2*-FGFR3c binding.

Table 1. Results of Model Fitting

	$\Delta G = -RT \ln K_1$ (kcal/mol)	$1/K_2$ (nM)
fgf1 titration experiment	−3.7 ± 0.4	0.2 ± 0.1
fgf2 titration experiment	−3.9 ± 0.4	2.2 ± 1.0

The optimal value of the dimerization constant K_1, obtained in the fit, was used to calculate the apparent free energy of ligand-independent dimerization, $\Delta G = -RT \ln K_1$. Two K_1 values were obtained in the two independent fits of the *fgf1* and *fgf2* data, and the respective free energies are shown in Table 1. The results pertain to the very same process, dimerization in the absence of ligand, and are thus expected to be the same. As seen in Table 1, the calculated dimerization free energies are indeed very similar, demonstrating the consistency of the data analysis.

DISCUSSION

Binding of *fgf1* and *fgf2* to subdomains D2 and D3 of FGFR3c extracellular domains has been measured previously in vitro using surface plasmon resonance.[20] These measurements revealed a difference in ligand binding strength: *fgf1* binding was stronger than *fgf2* binding. Such difference in binding was also observed using a soluble chimeric protein, consisting of FGFR3c extracellular domain fused to human placental alkaline phosphatase.[39] To investigate if such a difference is also observed for full-length FGFR3c, we measured FGFR3c phosphorylation over a wide ligand concentration range, and we fitted the model described by eqs 3−13 to these phosphorylation measurements. In our experiments we used a very broad range of ligand concentrations, including very high ligand concentrations, in order to determine the relevant parameters describing ligand binding. While the high ligand concentrations that we used here are not biologically relevant, this approach allowed us to compare not only the binding strengths of the two ligands to FGFR3c but also the relative ease of Y647/648 phosphorylation within the *fgf1* and *fgf2*-bound FGFR3c dimers. The conclusions that we drew based on these experiments pertain to the physical−chemical and biochemical characteristics of FGFR3c and thus should be always valid.

The experimental approach that we used here to monitor ligand binding was indirect, and the apparent ligand binding constant K_2 determined in the fit is not a direct measure of ligand binding affinity. Yet, this approach allowed us to monitor FGFR3c−ligand interactions that are productive (i.e., resulting in activation) such that the binding strengths of *fgf1* and *fgf2* can be compared in a biological context. We found that the apparent *fgf1*-FGFR3c dissociation constant is an order of magnitude lower than the *fgf2*-FGFR3c dissociation constant (see Table 1). Thus, our results are consistent with previous studies of the isolated extracellular domain,[20,39] confirming stronger binding for *fgf1* to FGFR3c, as compared to *fgf2*.

At high ligand concentrations, we observe a plateau in FGFR3c phosphorylation (Figures 3 and 5), similar to previous studies.[31] In the plateau, FGFR3c exists predominantly as liganded dimers,[31] and thus the difference at high ligand

concentrations can be attributed to the receptor phosphorylation levels in the liganded dimeric state. Our results showed that the receptor phosphorylation in the *fgf2*-bound dimers is exactly twice as high as the receptor phosphorylation in the *fgf1*-bound dimers (Figure 2). This intriguing finding demonstrates a different signaling capacity of FGFR3/*fgf1* and FGFR3/*fgf2* dimers.

RTK activation is known to require precise orientation and positioning of the catalytic domains with respect to each other, such that the phosphate group can be successfully transferred from ATP to the neighboring receptor. For EGFR, this entails the formation of an asymmetric kinase dimer in which the C-lobe of one kinase contacts the N-lobe of the second kinase and positions the activation loop of the second kinase to catalyze phosphate group transfer.[45] Similar asymmetric interactions have been proposed for FGF receptors.[46] A question remains, however, whether the two kinases alternate over time and act both as catalyst and substrate. Our finding that receptor phosphorylation levels in the *fgf2*-bound FGFR3c dimers are exactly twice as high as receptor phosphorylation levels in the *fgf1*-bound dimers may suggest that only one of the receptors is phosphorylated at Y647/8 in the *fgf1*-bound dimer, while both of them are phosphorylated in the *fgf2*-bound dimer. This implies that either the kinase structures and/or orientations in the *fgf1*-FGFR3c and *fgf2*-FGFR3c dimers are different or the conformational flexibilities are different in the two structures.

Perhaps the most interesting finding in this work is that the differences in ligand binding strength and in receptor phosphorylation levels in the liganded dimeric state compensate each other, such that the measured phosphorylation is similar at ligand concentrations below 500 ng/mL (or 30 nM) (Figure 3). The measured phosphorylation, however, is very different at higher ligand concentration. Thus, the ligand concentration range determines if the response to *fgf1* and *fgf2* is different or the same. This is a demonstration of the versatility of FGFR3c response to *fgf1* and *fgf2*. Note that FGFR3c plays a critical role during development, when one can expect large fluctuations in ligand expression. We can therefore expect that the differences in FGFR3c response to ligand that we report here are important for human development.

The finding that the measured FGFR3c phosphorylation is similar in response to low *fgf1* and *fgf2* concentrations (Figure 3) is consistent with previous results that the FGFR3c-mediated mitogenic activities of *fgf1* and *fgf2* are the same.[21] At first glance, these results seem to contradict the reports for different ligand binding strengths.[20,39] The presented work resolves the controversy, provides new knowledge about FGFR3c activation, and highlights the complexity in *fgf* signaling.

AUTHOR INFORMATION

Corresponding Author

*Tel: 410-516-8939. Fax: 410-516-5293. E-mail: kh@jhu.edu.

Funding

Supported by NIH GM068619.

ACKNOWLEDGMENTS

We thank Dr. Lijuan He for many useful discussions.

ABBREVIATIONS

FGFR3, fibroblast growth factor 3; fgf, fibroblast growth factor; HEK 293 T, human embryonic kidney 293 T.

REFERENCES

(1) Eswarakumar, V. P., Lax, I., and Schlessinger, J. (2005) Cellular signaling by fibroblast growth factor receptors. *Cytokine Growth Factor Rev. 16*, 139−149.

(2) Wilkie, A. O. M., Morriss-Kay, G. M., Jones, E. Y., and Heath, J. K. (1995) Functions of fibroblast growth factors and their receptors. *Curr. Biol. 5*, 500−507.

(3) Ornitz, D. M., and Itoh, N. (2001) Fibroblast growth factors. *Genome Biol.*, 2.

(4) GOSPODAR, D. (1974) Localization of A Fibroblast Growth-Factor and Its Effect Alone and with Hydrocortisone on 3T3 Cell-Growth. *Nature 249*, 123−127.

(5) Gospodarowicz, D. (1975) Purification of A Fibroblast Growth-Factor from Bovine Pituitary. *J. Biol. Chem. 250*, 2515−2520.

(6) Gospodarowicz, D., Bialecki, H., and Greenburg, G. (1978) Purification of Fibroblast Growth-Factor Activity from Bovine Brain. *J. Biol. Chem. 253*, 3736−3743.

(7) Maciag, T., Cerundolo, J., Ilsley, S., Kelley, P. R., and Forand, R. (1979) Endothelial Cell-Growth Factor from Bovine Hypothalamus - Identification and Partial Characterization. *Proc. Natl. Acad. Sci. U. S. A. 76*, 5674−5678.

(8) Mignatti, P., Morimoto, T., and Rifkin, D. B. (1992) Basic Fibroblast Growth-Factor, A Protein Devoid of Secretory Signal Sequence, Is Released by Cells Via A Pathway Independent of the Endoplasmic-Reticulum Golgi-Complex. *J. Cell. Physiol. 151*, 81−93.

(9) Prudovsky, I., Tarantini, F., Landriscina, M., Neivandt, D., Soldi, R., Kirov, A., Small, D., Kathir, K. M., Rajalingam, D., and Kumar, T. K. S. (2008) Secretion without Golgi. *J. Cell. Biochem. 103*, 1327−1343.

(10) Moscatelli, D. (1987) High and Low Affinity Binding-Sites for Basic Fibroblast Growth-Factor on Cultured-Cells - Absence of A Role for Low Affinity Binding in the Stimulation of Plasminogen-Activator Production by Bovine Capillary Endothelial-Cells. *J. Cell. Physiol. 131*, 123−130.

(11) Ornitz, D. M., Yayon, A., Flanagan, J. G., Svahn, C. M., Levi, E., and Leder, P. (1992) Heparin Is Required for Cell-Free Binding of Basic Fibroblast Growth-Factor to A Soluble Receptor and for Mitogenesis in Whole Cells. *Mol. Cell. Biol. 12*, 240−247.

(12) Yayon, A., Klagsbrun, M., Esko, J. D., Leder, P., and Ornitz, D. M. (1991) Cell-Surface, Heparin-Like Molecules Are Required for Binding of Basic Fibroblast Growth-Factor to Its High-Affinity Receptor. *Cell 64*, 841−848.

(13) Lin, X. H., Buff, E. M., Perrimon, N., and Michelson, A. M. (1999) Heparan sulfate proteoglycans are essential for FGF receptor signaling during Drosophila embryonic development. *Development 126*, 3715−3723.

(14) Plotnikov, A. N., Schlessinger, J., Hubbard, S. R., and Mohammadi, M. (1999) Structural basis for FGF receptor dimerization and activation. *Cell 98*, 641−650.

(15) Plotnikov, A. N., Hubbard, S. R., Schlessinger, J., and Mohammadi, M. (2000) Crystal structures of two FGF-FGFR complexes reveal the determinants of ligand-receptor specificity. *Cell 101*, 413−424.

(16) Mohammadi, M., Olsen, S. K., and Ibrahimi, O. A. (2005) Structural basis for fibroblast growth factor receptor activation. *Cytokine Growth Factor Rev. 16*, 107−137.

(17) Ornitz, D.M. (2000) FGFs, heparan sulfate and FGFRs: complex interactions essential for development. *BioEssays 22*, 108−112.

(18) L'Horte, C. G. M., and Knowles, M. A. (2005) Cell responses to FGFR3 signaling: growth, differentiation and apoptosis. Experim. *Cell Res. 304*, 417−431.

(19) Ibrahimi, O. A., Zhang, F. M., Eliseenkova, A. V., Itoh, N., Linhardt, R. J., and Mohammadi, M. (2004) Biochemical analysis of pathogenic ligand-dependent FGFR2 mutations suggests distinct pathophysiological mechanisms for craniofacial and limb abnormalities. *Hum. Mol. Genet. 13*, 2313−2324.

(20) Ibrahimi, O.A., Zhang, F. M., Eliseenkova, A. V., Linhardt, R. J., and Mohammadi, M. (2004) Proline to arginine mutations in FGF receptors 1 and 3 result in Pfeiffer and Muenke craniosynostosis

syndromes through enhancement of FGF binding affinity. *Hum. Mol. Genet. 13*, 69−78.
(21) Ornitz, D. M., Xu, J. S., Colvin, J. S., Mcewen, D. G., MacArthur, C. A., Coulier, F., Gao, G. X., and Goldfarb, M. (1996) Receptor specificity of the fibroblast growth factor family. *J. Biol. Chem. 271*, 15292−15297.
(22) Zhang, X. Q., Ibrahimi, O. A., Olsen, S. K., Umemori, H., Mohammadi, M., and Ornitz, D. M. (2006) Receptor specificity of the fibroblast growth factor family - The complete mammalian FGF family. *J. Biol. Chem. 281*, 15694−15700.
(23) Olsen, S. K., Ibrahimi, O. A., Raucci, A., Zhang, F. M., Eliseenkova, A. V., Yayon, A., Basilico, C., Linhardt, R. J., Schlessinger, J., and Mohammadi, M. (2004) Insights into the molecular basis for fibroblast growth factor receptor autoinhibition and ligand-binding promiscuity. *Proc. Natl. Acad. Sci. U. S. A. 101*, 935−940.
(24) Radvanyi, F., Thiery, J. P., Billerey, C., van derKwast, T. H., Zafrani, E. S., and Chopin, D. (2001) Fibroblast growth factor receptor: from chondrodysplasia to bladder cancer. *M S-Med. Sci. 17*, 1189−1191.
(25) Vajo, Z., Francomano, C. A., and Wilkin, D. J. (2000) The molecular and genetic basis of fibroblast growth factor receptor 3 disorders: The achondroplasia family of skeletal dysplasias, Muenke craniosynostosis, and Crouzon syndrome with acanthosis nigricans. *Endocrine Rev. 21*, 23−39.
(26) Shiang, R., Thompson, L. M., Zhu, Y.-Z., Church, D. M., Fielder, T. J., Bocian, M., Winokur, S. T., and Wasmuth, J. J. (1994) Mutations in the transmembrane domain of FGFR3 cause the most common genetic form of dwarfism, achondroplasia. *Cell 78*, 335−342.
(27) Bellus, G. A., Mcintosh, I., Smith, E. A., Aylsworth, A. S., Kaitila, I., Horton, W. A., Greenhaw, G. A., Hecht, J. T., and Francomano, C. A. (1995) A Recurrent Mutation in the Tyrosine Kinase Domain of Fibroblast Growth-Factor Receptor-3 Causes Hypochondroplasia. *Nature Genet. 10*, 357−359.
(28) Naski, M. C., Wang, Q., Xu, J. S., and Ornitz, D. M. (1996) Graded activation of fibroblast growth factor receptor 3 by mutations causing achondroplasia and thanatophoric dysplasia. *Nature Genet. 13*, 233−237.
(29) Cho, J. Y., Guo, C. S., Torello, M., Lunstrum, G. P., Iwata, T., Deng, C. X., and Horton, W. A. (2004) Defective lysosomal targeting of activated fibroblast growth factor receptor 3 in achondroplasia. *Proc. Natl. Acad. Sci. U. S. A. 101*, 609−614.
(30) Guo, C. S., Degnin, C. R., Laederich, M. B., Lunstrum, G. P., Holden, P., Bihimaier, J., Krakow, D., Cho, Y. J., and Horton, W. A. (2008) Sprouty 2 disturbs FGFR3 degradation in thanatophoric dysplasia type II: A severe form of human achondroplasia. *Cell. Signalling 20*, 1471−1477.
(31) He, L., Horton, W. A., and Hristova, K. (2010) The physical basis behind achondroplasia, the most common form of human dwarfism. *J. Biol. Chem. 285*, 30103−30114.
(32) Li, E., You, M., and Hristova, K. (2006) FGFR3 dimer stabilization due to a single amino acid pathogenic mutation. *J. Mol. Biol. 356*, 600−612.
(33) You, M., Spangler, J., Li, E., Han, X., Ghosh, P., and Hristova, K. (2007) Effect of pathogenic cysteine mutations on FGFR3 transmembrane domain dimerization in detergents and lipid bilayers. *Biochemistry 46*, 11039−11046.
(34) You, M., Li, E., and Hristova, K. (2006) The achondroplasia mutation does not alter the dimerization energetics of FGFR3 transmembrane domain. *Biochemistry 45*, 5551−5556.
(35) Monsonego-Ornan, E., Adar, R., Feferman, T., Segev, O., and Yayon, A. (2000) The transmembrane mutation G380R in fibroblast growth factor receptor 3 uncouples ligand-mediated receptor activation from down-regulation. *Mol. Cell. Biol. 20*, 516−522.
(36) Monsonego-Ornan, E., Adar, R., Rom, E., and Yayon, A. (2002) FGF receptors ubiquitylation: dependence on tyrosine kinase activity and role in downregulation. *FEBS Lett. 528*, 83−89.
(37) Adar, R., Monsonego-Ornan, E., David, P., and Yayon, A. (2002) Differential activation of cysteine-substitution mutants of fibroblast growth factor receptor 3 is determined by cysteine localization. *J. Bone Miner. Res. 17*, 860−868.
(38) He, L., Wimley, W. C., and Hristova, K. (2011) FGFR3 heterodimerization in achondroplasia, the most common form of human dwarfism. *J. Biol. Chem. 286*, 13272−13281.
(39) Chellaiah, A., Yuan, W. L., Chellaiah, M., and Ornitz, D. M. (1999) Mapping ligand binding domains in chimeric fibroblast growth factor receptor molecules - Multiple regions determine ligand binding specificity. *J. Biol. Chem. 274*, 34785−34794.
(40) He, L., and Hristova, K. (2008) Pathogenic activation of receptor tyrosine kinases in mammalian membranes. *J. Mol. Biol. 384*, 1130−1142.
(41) Harmer, N. J. (2006) Insights into the role of heparan sulphate in fibroblast growth factor signalling. *Biochem. Soc. Trans. 34*, 442−445.
(42) Chen, F., Degnin, C., Laederich, M. B., Horton, A. W., and Hristova, K. (2011) The A391E mutation enhances FGFR3 activation in the absence of ligand. *Biochim. Biophys. Acta, Biomembr. 1808*, 2045−2050.
(43) Mohammadi, M., Dikic, I., Sorokin, A., Burgess, W. H., Jaye, M., and Schlessinger, J. (1996) Identification of six novel autophosphorylation sites on fibroblast growth factor receptor 1 and elucidation of their importance in receptor activation and signal transduction. *Mol. Cell. Biol. 16*, 977−989.
(44) Raffioni, S., Zhu, Y. Z., Bradshaw, R. A., and Thompson, L. M. (1998) Effect of transmembrane and kinase domain mutations on fibroblast growth factor receptor 3 chimera signaling in PC12 cells. A model for the control of receptor tyrosine kinase activation. *J. Biol. Chem. 273*, 35250−35259.
(45) Zhang, X. W., Gureasko, J., Shen, K., Cole, P. A., and Kuriyan, J. (2006) An allosteric mechanism for activation of the kinase domain of epidermal growth factor receptor. *Cell 125*, 1137−1149.
(46) Bae, J. H., Boggon, T. J., Tome, F., Mandiyan, V., Lax, I., and Schlessinger, J. (2010) Asymmetric receptor contact is required for tyrosine autophosphorylation of fibroblast growth factor receptor in living cells. *Proc. Natl. Acad. Sci. U. S. A. 107*, 2866−2871.